The Pennsylvania State University

The Graduate School

College of Engineering

CONTROLLING THE ADSORPTION OF PROTEINS ON POLY(P-XYLYLENE) POLYMERIC THIN FILMS

A Thesis in

Engineering Science

by

Michael K. Anderson

Submitted in Partial Fulfillment
of the Requirements
for the Degree of

Master of Science

May 2010

The thesis of Michael K. Anderson was reviewed and approved* by the following:

Melik C. Demirel
Associate Professor of Engineering Science and Mechanics
Thesis Adviser

Srinivas Tadigadapa
Associate Professor of Electrical Engineering

Tony Jun Huang
James Henderson Assistant Professor of Engineering Science and Mechanics

Judith Todd
P.B. Breneman Department Head Chair
Head of the Department of Engineering Science and Mechanics

*Signatures are on file in the Graduate School

Abstract

In order to control the interactions of biomolecules and surfaces, first the adsorption of proteins to that surface must be controlled. This study investigates the use of poly(p-xylylene) (PPX), a polymer with the capacity for design on the nanoscale, as a way of controlling protein adsorption. By altering the morphology and thus the surface area of the polymer, protein adsorption is able to be controlled in a predictable fashion. This study also looks at the use Quartz Crystal Microbalance to measure frequency shift and resistance and thus to gain information on the protein adsorption and the character of such adsorption. Protein adsorption data is reported for a model protein (i.e., Bovine Serum Albumin (BSA)) on three different morphologies of PPX. Due to ~420% and ~450% increases respectively in surface area over planar PPX, helical and columnar samples of PPX enhance protein adsorption affinity by ~800% and ~700% respectively over planar PPX.

Acknowledgements

I would like to begin by first acknowledging God, who through the gospel of Jesus Christ has given me confidence and assurance before Him. It is only out of that confidence and assurance that I am able to move forward into any difficult task, knowing that my relative success or failure does not determine my standing before Him. The completion of this thesis is a result of that truth. I would also like to thank my parents for loving me as long as I have been alive and for providing me with the opportunity to attend Penn State and carry out such work as this. As for my lab team, while I have received much help from different sources, I would specifically like to acknowledge Dr. Melik Demirel, Dr. Hui Wang, Dr. Gohkan Demirel, and Niranjan Malvadkar. As my thesis advisor, Dr. Melik Demirel gave me the idea for this project and equipped me with the science to understand it. Dr. Hui Wang worked patiently with me through many failures on my part as he explained and demonstrated how to be a good experimentalist. Dr. Gohkan Demirel took time out of his busy schedule on many occasions to offer his expertise in surface chemistry and his advice throughout the process was invaluable to the success of this work. Niranjan Malvadkar introduced me to the experimental methods necessary to complete this work and the relevant literature. He also patiently helped me evaluate my data and his expertise proved to be an invaluable part of this research. I thank God for all of these people and for the opportunity to do this research.

Table of Contents

Acknowledgements....iv

List of Figures....vi

List of Tables....vii

List of Equations....viii

Chapter 1: Introduction....1

1.1 - Overview and Problem Statement....1

1.2 - Literature Review....4

1.2.1 - Design and Production of Poly-(p-xylylene) (PPX)....4

1.2.2 - Quartz Crystal Microbalance: Theory and Use in Protein Adsorption....9

1.3 - Methodology....17

Chapter 2: Results....20

2.1 - Data....20

2.2 - Discussion....26

Chapter 3: Conclusion....31

References....33

List of Figures

Figure 1: Oblique Angle Deposition Schematic.....6

Figure 2: Butterworth-Van Dyke Equivalent Circuit Model.....10

Figure 3: Frequency over Time QCM Measurement Example.....20

Figure 4: PPX-Cl BSA Adsorption Isotherms.....21

Figure 5: PPX-Cl Langmuir Fitting.....22

Figure 6: Resistance Changes in BSA Adsorption.....24

Figure 7: Resistance Effects on Frequency Shift.....25

List of Tables

Table 1: PPX-Cl Thickness for Different Morphologies.....18

Table 2: PPX-Cl Langmuir Fitting Values.....23

Table 3: PPX-Cl Surface area and Langmuir Constant Comparison.....23

List of Equations

Equation 1: Sauerbrey Equation.....9

Equation 2: Kanazawa Equation.....10

Equation 3: Frequency Shift for R-QCM.....11

Equation 4: Equivalent Resistance Shift for R-QCM.....11

Equation 5: Langmuir Equation.....12

Chapter 1: Introduction

1.1 Overview and Problem Statement

While protein adsorption has been an area of study for some time now, over the last forty years there has been a growing interest in protein adsorption to polymers due to the potential of using such polymers in biomedical devices. Protein adsorption is the first step in understanding the interaction of biomolecules and surfaces. Thus to control the interaction between biomolecules and a surface, controlling protein adsorption is an important factor [1]. To control protein adsorption, the properties of a surface must have the capacity to be changed in such a way as to produce a predictable pattern of protein adsorption. This study presents the use of a nanoporous polymer with tunable surface morphology to control protein adsorption.

The polymer used in this experiment is poly-(p-xylylene) (PPX). It is created from a [2,2]paracyclophane precursor commercially named Parylene and deposited using chemical and physical vapor deposition methods. This material is attractive as a controlled release platform because of its nanoengineering capacity, easily alterable surface properties, and the possibility of growing various polymer brushes on its surface. Through use of glancing angle deposition, various PPX features can be engineering on the nanoscale such as columns, helices, and zig-zags [2]. The presence of increased surface area and spacing between features lends itself to the possibility of molecules embedding between the features. The adsorption is then to occur by a protein adsorbing between the features. This study tests the validity of such an approach to controlling protein adsorption by comparing the protein adsorption of nanostructured surfaces to that of their planar counterparts.

Another aspect of this research is the use of a Quartz Crystal Microbalance (QCM) to study drug loading via measurements of protein adsorption. QCM in general contains two electrodes on either side of disk coated with some type of quartz. When a voltage is applied across the electrodes, it causes a shear deformation. When that voltage is at a certain excitation frequency, it causes a standing shear wave to form along the thickness of the plate. Sauerbrey et. al. showed that changes in the resonant frequency of that standing shear wave are directly proportional to the mass loading on that surface [3]. Martin et. al. further demonstrated that both liquid and mass loading properties can be determined to a high degree of sensitivity using QCM [4]. This makes it an attractive option to measure loading on PPX while in a liquid solution. Since the affects of surface chemistry on protein adsorption has already received some attention, this study focused on how to control adsorption or loading by alterations of the surface morphology of the nanostructures.

If successful, this work would provide a reproducible method to control protein adsorption and thus biomolecular interactions. Probably the best known application of controlled protein adsorption is for biomedical devices for the cardiovascular system, since protein adsorption is a determining factor in controlling blood coagulation and complement activation. Cell adhesion is also mediated by an interlayer of adsorbed protein [1]. If it could be patterned in the future it could then be used for cell patterning applications where a template could be designed that would grow cells at predetermined concentrations and locations. Such control over cell/surface interactions and over other biomolecules similar to proteins would also make it an attractive option for controlled drug delivery systems where specific adsorption and release is required. A similar

benefit could be exposed in tissue engineering where often growth factor must be loaded and released in a controlled fashion from a polymer scaffold.

1.2 - Literature Review

1.2.1 - Design and Production of Poly-(p-xylylene) (PPX)

In this research, the material exclusively studied was poly-(p-xylylene), hereafter referred to simply as PPX, a polymer deposited using a nanotechnology application of physical vapor deposition. The following outlines the research leading to the production of "nanostructured" PPX films.

Oblique angle deposition, also known as glancing angle deposition (GLAD), is a method of physical vapor deposition in which the normal of the substrate is tilted at some angle relative to the incident vapor flux. The earliest reported study into oblique angle deposition was by Kundt in 1886 [5]. Kundt's original idea that the anisotropy of such films were caused by the morphology was later verified with improved characterization methods such as electron microscopy [6]. Konig and Helwig used such characterization tools in the 1950's to show that the morphology of the films was controlled by the process of self-shadowing, also known as atomic-scale shadowing [7].

The process of self-shadowing is due in part to the properties of physical vapor deposition. Physical vapor deposition is a process by which a material is deposited onto a substrate. It is physical in nature since the material being deposited onto the substrate does not undergo any reaction with the substrate, which is the case in chemical vapor deposition. The vapor is instead deposited on the surface via condensation where while the vapor is being deposited it is in the gas phase but once arriving on the substrate, begins to undergo a phase transformation into the solid phase [6].

The flow of the vapor onto the surface is the incident vapor flux. As the incident vapor flux makes contact with the surface, the atoms diffuse in a random manner over the

substrate. The atoms that diffuse will continue to do so until stopped by either nucleation or reevaporation. Nucleation is the process by which nuclei of a new phase form and facilitate the process of phase transformation. Nucleation will not occur for all atoms deposited onto the surface, but only for atoms for which the Gibbs free energy of the system will be lowered by nucleation. The atoms that do not meet this criterion can simply reevaporate from the surface [9].

Once nucleation occurs, growth can begin. While there are three main growth mechanisms, the one most important in oblique angle deposition is the Volmer-Weber growth mode. In the Volmer-Weber growth mode, atoms deposited on the surface are more attracted to themselves than they are to the surface, causing three-dimensional nuclei to form. Since the atoms are more attracted to themselves than to the substrate, nucleation and growth of newly deposited atoms will tend to occur at sites where nucleation has already begun [6].

It is this principle then that leads to self-shadowing in oblique angle deposition. As atoms continue to be deposited onto the substrate, existing nuclei will intercept that vapor, thereby "shadowing" it from reaching nearby un-nucleated sites. As growth continues in already nucleated sites, shadowing will only increase. The shadowing then leads to columnar structures tilted at some angle relative to the incident vapor flux. Once formed the films undergo some columnar evolution. Since the shadowed areas of the material are not receiving any vapor, they will eventually become extinct, decreasing planar density. To compensate for that decrease in planar density, the non-shadowed columns that have been receiving flux will increase in diameter [6].

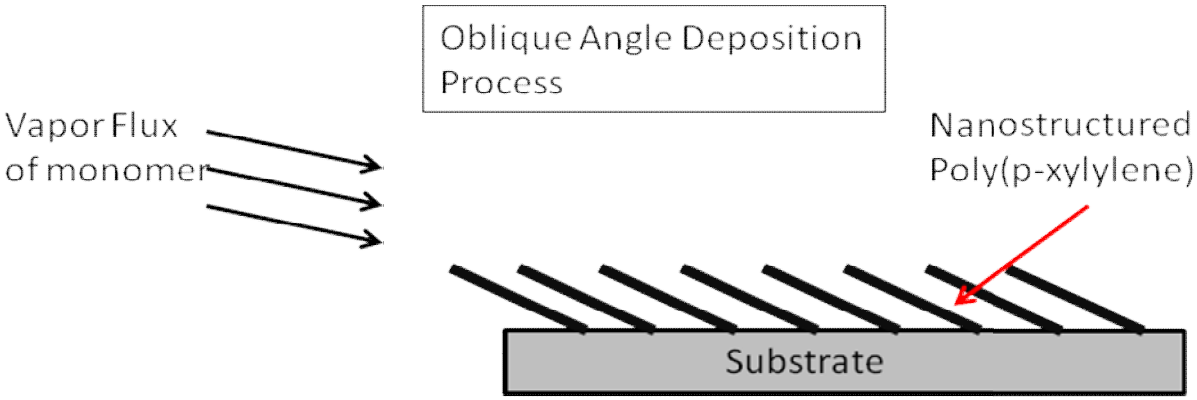

Figure 1 - Schematic representation of the oblique angle deposition process. Figure adapted from [9]

Later Demirel et al. used oblique angle deposition to deposit a polymer. The basic concept of that deposition is shown in Figure 1. That experiment began with a [2,2]paracyclophane. The [2,2]paracyclophane was then placed in a machine which first heated it to the point where it sublimated from the solid state to the gaseous state and then heated it more to the point where the bond connecting the two benzene rings of the dimer were broken into two reactive monomers. Each monomer contained a benzene ring, a chlorine functional group, and two terminal carbon radicals, one on each end. Once these reactive monomers were then deposited onto a substrate under the proper conditions, they could polymerize and nucleation ensued. The substrate was rotated such that helical structures formed at oblique angles, exhibiting the same results in morphology that oblique angle deposition did historically for metals [9, 10].

Further research went on to confirm that [2,2]paracylophanes of many different functional groups could be deposited using this method to form planar structures which are deposited with the incident vapor flux parallel to the substrate normal, columnar structures formed at some angle by oblique angle deposition, and helical structures formed by rotating the substrate. The film produced was a poly(p-xylylene) (PPX) and

any version of it deposited either at some angle relative to the substrate normal or while rotating the substrate was called a structured film [11].

While films prepared using oblique angle deposition have a number of applications, one that proved particularly useful was the increased surface area of structured films versus their planar counterparts. As the size of columns decreases to the nanoscale as is the case in Demirel's research, the same amount of mass as in a planar structure is now distributed to small columnar structures, thereby increasing the surface area. This property has been put to use in the production of solar cells, solid oxide fuel cells, and sensor devices. One of the most useful applications of increased surface area of a solid in general its increase in potentially active sites [6].

The Demirel lab further exploited this property in an experiment functionalizing PPX films with a Green Fluorescent Protein (GFP). This experiment did in fact conclude that structured PPX films were more readily functionalized with GFP than their planar counterparts due to the increased surface area of structured films [12]. Surface area was further studied and quantified in the thesis work of Purcell, where it was found that surface area was largest for the helical morphology, then lesser for the columnar morphology, and least for the planar morphology [13]. Also an important factor for biological applications, PPX exhibited some level of biocompatibility when Demirel et. al. were able to attach and grow fibroblast cells on PPX films [9].

The combined weight of this research is to establish that PPX can be deposited using physical vapor deposition, can be engineered on the nanoscale using oblique angle deposition, and can possibly entrap proteins or drugs in between its nanostructures. Its surface morphology is also easily controlled by the deposition conditions. The ability to

change such surface morphologies will be tested as a way of controlling protein adsorption.

1.2.2 - Quartz Crystal Microbalance: Theory and Use in Protein Adsorption

A Quartz Crystal Microbalance (QCM) is a device used to measure changes at the interface of some surface. It does this through use of a piezoelectric quartz crystal, normally an AT-cut single-crystal quartz wafer. This crystal is deposited on some thin plate with two electrodes on either end of the crystal. As a voltage is applied across the electrodes, the piezoelectric properties of the quartz crystal cause a shear deformation. When that voltage is at a certain excitation frequency, it causes a standing shear wave to form along the thickness of the plate. Sauerbrey et. al. showed that the frequency of this standing shear wave was directly proportional to the change in mass present on the surface. Sauerbrey quantified this relationship through the Sauerbrey equation:

$$\Delta f_s^{mass} = -\left(\frac{2 f_s^2}{\sqrt{\bar{c}_{66} \rho_Q}} \right) \times \rho_s \quad \text{(Equation 1)}$$

where f_s, is the first-harmonic resonant frequency $\bar{c}_{66}$ is the piezoelectric constant and ρ_Q is the density of the quartz crystal, and ρ_s is the surface density of deposited mass. This equation assumes no energy loss and is thus only valid for purely rigid adsorption in vacuum. As mass accumulates on the surface due to deposition, the QCM measures changes in frequency that correspond to those changes in mass [3].

The use of QCM broadened when in the 1980s it was shown that QCM could operate under liquid loading. However, a difficulty that soon arose was interpreting the changes in resonant frequency in the liquid loading situation. Whereas in vacuum conditions as in those studied by Sauerbrey, a change in resonant frequency simply corresponded to a change in mass on the surface, Kanazawa and Gordon soon showed that no longer was the case for liquid loading. Since the liquid is viscously coupled to the

surface of the quartz crystal, it leads to a damping of the resonant frequency. They derived an equation quantifying the frequency shift under liquid loading conditions [14].

$$\Delta f_s^{liquid} = -\left(\frac{f_s^{3/2}}{\sqrt{\pi \bar{c}_{66} \rho_Q}} \right) \times \sqrt{\rho_L \eta_L} \quad \text{(Equation 2)}$$

Kanazawa's study thus proved that measuring only the resonant frequency under liquid loading conditions would be insufficient to determine how much mass was actually present on the crystal's surface. Later however Martin et. al. sought to quantify the effects of simultaneous liquid and mass loading. They found the total frequency shift is essentially the algebraic sum of Kanazawa's and Sauerbrey's equations.

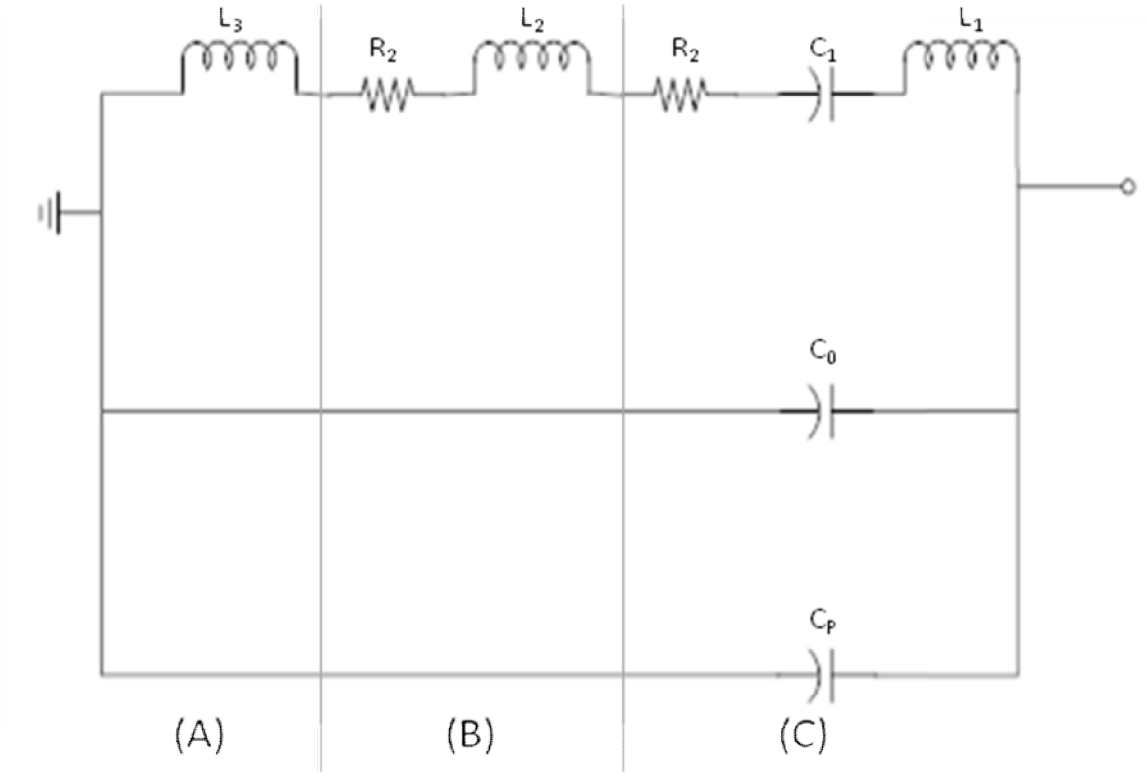

Figure 2 - Modified Butterworth-Van Dyke equivalent circuit model for simultaneous mass and liquid loading. Region A represents the effect from mass loading, region B the effect from liquid loading, region C that of the bare crystal. Figure adapted from [4].

They also developed a continuum electromechanical model using a modified Butterworth-Van-Dyke equivalent circuit model (Figure 3). C_1, R_1, and L_1 are simply the

motional capacitance, resistance, and inductance respectively of the QCM crystal with no loading. C_0 represents the static capacitance while C_P denotes what they call "parasitic capacitance," a capacitance arising from varying geometry and electrode location on the QCM crystal. The RQCM used in this experiment cancels C_0 and C_P before data points are recorded through use of a varactor diode. In the case of liquid loading, they observed an interfacial resistance to shear deformation. Since shear deformation is what causes a frequency shift, this resistance to shear deformation is what causes there to be a frequency shift even when there is no actual mass loading. This is a representation of the previously observed phenomena of viscous coupling. R_2 and L_2 account for this resistance and will be used to determine the contribution of viscous coupling to frequency shift. L_3 accounts for actual mass loading similar to that represented by Sauerbrey's equation (Equation 1). By solving this model, they were able to derive analytic expressions for their parameters [4].

The QCM used in this study (Maxtek RQCM, Inficon Inc., NY) measures simultaneously the frequency shift and the resistance (R_2) in such an equivalent circuit model. Combining Martin's results and the measurements taken by the QCM used in this study gives the following equations for the frequency shift and change in resistance:

$$\Delta f_s = -f_s\left(\frac{L_2 + L_3}{2\sum_{1,2,3} L_n}\right) \approx -\frac{2 f_s^{\,2}}{\sqrt{\bar{c}_{66}\rho_Q}}\left(\rho_s + \left(\frac{\rho_L \eta_L}{4\pi f_s}\right)^{1/2}\right) \quad \text{(Equation 3)}$$

$$\Delta R = \left(R_1 + R_2\right) - R_1 = R_2 = \frac{\omega_s L_1}{N\pi}\sqrt{\frac{2\omega\rho_L\eta_L}{\bar{c}_{66}\rho_Q}} \quad \text{(Equation 4)}$$

It is important to note at this point that the models described here only apply for a certain penetration depth of the liquid that the nanostructured polymer exceeds. Because

of the nanostructures and the order of thickness of the film, the model cannot be known to apply strictly to this case. However it is assumed for the purposes of this study that the polymer coating oscillates in unison with the crystal. Therefore the entire surface of the nanostructures is considered to be the surface represented by the aforementioned models.

One of the key features of the QCM for this study was the ability to measure protein adsorption. The application of QCM explored in this review will then focus on its use in measuring adsorption. Before reviewing the work in using QCM to measure protein adsorption, a brief note on protein adsorption is in order. The protein adsorption model used in this study to model the adsorption of BSA comes from the work of Irvin Langmuir. In 1916 Langmuir published an extensive paper in which he puts forth an equation describing the adsorption of proteins onto a surface known as the Langmuir equation. The protein adsorption he used this equation to describe followed the general pattern of an initially large increase in adsorption compared to an eventual plateau of adsorption at the saturation point. The version of the Langmuir equation used in this study is as follows:

$$\Gamma = \Gamma_{max} \frac{Kc}{1 + Kc} \quad \text{(Equation 5)}$$

Where Γ represents amount of mass adsorbed, Γ_{max} represents the largest recorded adsorbed mass, K represents the equilibrium constant for the adsorption of protein, hereafter referred to simply as the Langmuir constant and c represents the concentration of the test solution. Since K represents the equilibrium constant for the adsorption of the protein, it can also be thought of as a way of measuring adsorption affinity [15].

In 2003 Marxer et. al. studied the adsorption of Protein A-BSA-IgG and Fibronectin on gold and tin surfaces using QCM. The QCM measured changes in

resonant frequency that corresponds to mass changes. They separated out the effects of the liquid properties by measuring the oscillation amplitude and dissipation factor. Particularly relevant for this study, they found that BSA does affect the viscous properties of solvents such that it is partially responsible for frequency shifts. This shows the importance of measuring in some way the effects of the solvent properties when studying the adsorption of BSA. When they measured adsorption of BSA, they did so only after first adsorbing a layer of Protein A on the surface. They saw that the adsorption of BSA was inversely proportional to the adsorption of Protein A. This is because as Protein A covers the surface, BSA has less vacant sites on which to adsorb. In their study of the rigidity of adsorption, two observations are particularly relevant. They observe more rigid adsorption for the gold surface than the titanium surface, and at one point even observe a decrease in dissipation factor between data points on gold. They attribute the more rigid adsorption on gold to the fact that there are more proteins present on its surface and therefore more water is expelled. They explain the decrease in dissipation factor between data points for the gold surface to the rigidifying of the layer. They also observed the effects of using phosphate and buffer solutions with salt ions as a solvent for the proteins they studied. In adsorption, they noted that salt ions can affect the frequency shifts recorded, so that must be taken into consideration when using such a solvent in protein adsorption studies [16].

In 2004 Perry et. al. studied BSA and fibrinogen adsorption in an attempt to interpret the effects of surface chemistry on protein adsorption, specifically in terms of how it relates to the conformation of adsorbed protein. They use QCM to measure rates of adsorption and the amount of proteins adsorb while using Grazing Angle Infrared

Spectroscopy (GA-FTIR) to obtain information about the conformation of the protein upon adsorption. They tested the adsorption of these two proteins onto both CH_3 and OH terminated surfaces, or hydrophobic and hydrophilic surfaces, respectively. They found that in both cases as they increased the protein loading concentration, the frequency shift and rate of increase in frequency shift increased. For each concentration this occurs until the adsorption reaches an equilibrium where the rate of adsorption and desorption are equivalent. At that point the frequency shift stops increasing. This continued until at higher concentrations the frequency shift ceased to increase. This is the point at which the surface is fully saturated with proteins. They found BSA to have a stronger adsorption affinity for the hydrophobic surface through comparing the Langmuir adsorption constants. However, BSA achieves a greater final surface coverage on a hydrophilic surface. They attribute this to the fact that BSA undergoes conformational changes to adsorb to a hydrophobic surface, creating a great affinity for a hydrophobic surface but also taking up more surface area on a hydrophobic surface, inhibiting further adsorption. Their use of GA-FTIR to study conformation revealed some information on the mechanism of BSA adsorption. Essentially the BSA undergoes a conformational shift to expose its hydrophobic parts to the hydrophobic surface and expel water in an energetically favorable transaction. It is thus expected that BSA will prefer adsorption to hydrophobic surfaces for this reason. This study also shows the validity and use of QCM to measure adsorption amounts and rates [17].

In 2007 Kaufman et. al. studied the adsorption of three proteins including BSA on self-assembled monolayers of mercaptoundecanoic acid (MUA) on gold nanoparticles and bulk gold. They used QCM with dissipation measurements to measure the protein

adsorption. They also applied a Langmuir model to estimate binding constants, but they did say the model breaks down at points of their data and is therefore only to be viewed as a relative value to compare binding between different scenarios. In the BSA tests they measured protein adsorption both before rinsing and after rinsing to determine what of the protein was irreversibly adsorbed. The pre-rinse data seems to suggest the formation of multiple layers of BSA, but after rinsing there does not appear to be much BSA on the surface. To determine the effects of the liquid properties on this, they studied BSA concentration's effect on density and viscosity, and how that then impacts QCM measurements. They concluded that changes in density and viscosity caused by changing the concentration of BSA do not have a significant impact on QCM measurements under 25 μM concentrations of BSA. They see that changes in frequency above this concentration are due to changes in the liquid viscosity and density. By comparing pre-rinse and post-rinse data they conclude that in their study BSA adsorbs by a single rigid layer and a second loosely bound surface aggregate layer that is easily desorbed by rinsing [18].

In 2008, Tadigadapa et. al. published work on the use of QCM to measure protein adsorption. While much QCM work uses crystals with fundamental frequencies of a lower value, they designed a QCM system using crystals with fundamental frequencies in the range of 62 MHz. They tested the adsorption of Human Serum Albumin (HSA) to demonstrate the effectiveness of such a method. The values of the Langmuir constant from the isotherms comparing the frequency shift to bulk protein concentration matched reasonably well the previous literature, thus validating this technique for measurement of protein adsorption and Langmuir fitting [19]. They later showed that such a technique

was reproducible for other proteins such as Immunoglobin G (IgG) as Langmuir fitting continued to yield values that match previous literature [20]. While this study uses quartz crystal with a fundamental frequency of roughly 5 MHz, this work does show the repeated valid use of QCM as a method to measure protein adsorption.

This section of the review demonstrates that QCM can and has been successfully used to measure protein adsorption by measuring frequency shifts. It also explains the use of resistance to determine the effects of liquid loading on these frequency shifts. Langmuir adsorption was also described briefly as the method used to describe the protein adsorption in this study.

1.3 - Methodology

The deposition process takes on the same general form for each different film tested. Each film is developed by starting with parylene. Parylene is the commercial name for a variety of poly(p-xylylene) polymers. The one used in this case is poly-p-(xylylene), derived from a [2,2]paracyclophane precursor version of parylene, hereafter referred to simply as PPX. PPX can be deposited with a variety of functional groups, although in this experiment only a chloro functionality was tested. These functional groups are attached to the initial dimer used for the deposition. When one of those functional groups is attached, it will be labeled as such in the results section.

All depositions are performed in a commercial PPX reactor. The process begins by placing solid amounts of the parylene sample into an evacuated chamber in their natural dimer form. Via high temperature pyrolysis, the dimer is converted into a reactive monomer vapor. The vapor is then directed onto a substrate through a nozzle. The substrate is a Si (100) wafer that has been successively emerged in HCl/CH_3OH (1:1 v/v), deionized water, and concentrated H_2SO_4. This wafer then has deposited on it a self-assembled organosilane monolayer. When the parylene monomer vapor hits the substrate, it condenses and polymerizes. The morphology is determined from the angle the substrate is placed at with respect to the nozzle that the vapor comes out of. For a columnar film, the substrate is at a 10 degree angle, for helical films the substrate is at 10 degrees and is continuously rotated, and for the planar film no nozzle is used so that the vapor deposits itself without any nanostructure.

For QCM studies, the first step taken was to deposit the films. A 5 MHz crystal with gold electrodes (QCM-100, SRS Inc., CA) was soaked in octadecanethiol (C18-

thiol) overnight to deposit a self-assembled monolayer (SAM) on the surface. After attachment of the SAM the crystal was rinsed with ethanol and dried. It was then placed in the PPX deposition machine and underwent the same deposition process described above. For these depositions, .3 g of PPX-Cl was placed in the evacuation chamber for helical and columnar samples while 3 g of PPX-Cl was used for planar samples. Profilometry results give the following thicknesses for helical, columnar, and planar morphologies deposited with the masses just given.

Film Type	Mass (g)	Thickness (μm)
PPX-Cl Helical	0.3	6.19
PPX-Cl Columnar	3	7.1
PPX-Cl Planar	3	4.445

Table 1 – Film thicknesses for different PPX-Cl morphologies. The thicknesses given are average thicknesses as the thickness varies over the entire surface.

. BSA solutions of .072, .289, 1.44, 2.89, 14.43, 28.9, 72.13, and 144.25 μM were prepared by dissolving BSA in Phosphate Buffered Saline (PBS) at room temperature. PBS was prepared through dissolving PBS tables (OmniPur, EMD Chemicals, Inc., NJ) in distilled water. One PBS tablet was dissolved per 100 mL of water to make a 1x PBS solution.

The quartz crystals with PPX deposited were then placed in a crystal holder (Maxtek Inc., NY). The crystal holder was attached to the R-QCM machine (Maxtek Inc., NY) via an SMB cable. The R-QCM recorded the frequency, change in frequency, and resistance at set time intervals. Adsorption measurements were taken by first placing the holder with the crystal in the beaker with pure PBS solution. Once the measured frequency reached a stable equilibrium, the holder was removed from PBS and placed into a beaker containing BSA solution of some known concentration being tested. In each case the holder and crystal were completely submerged in the test solution.

To develop the isotherms, the frequency change for each concentration was considered. That frequency change is measured from the final equilibrium frequency of the previous concentration to the final equilibrium frequency of the concentration tested. That is then plotted against concentration. The change in resistance is determined similarly and plotted against the change in frequency for each sample.

The surface area values reported were obtained previously using a Micromeritics' ASAP 2020 Accelerated Surface Area and Porosimetry analyzer [21].

Results

2.1 - Data

QCM was used to measure frequency shifts and changes in resistance for BSA adsorption studies of different morphologies of PPX. First frequency shift was studied since a negative frequency shift is directly related to mass loading. The QCM used was able to detect a consistent frequency and record these frequency values over long enough time intervals until the frequency drop reached equilibrium. Equilibrium was taken to be the time at which the frequency is decrease less than 1 Hz in an hour. Below is an example of the frequency shift measurements taken by the QCM over a time interval until equilibrium. Only one graph is shown to simply illustrate the validity of the method.

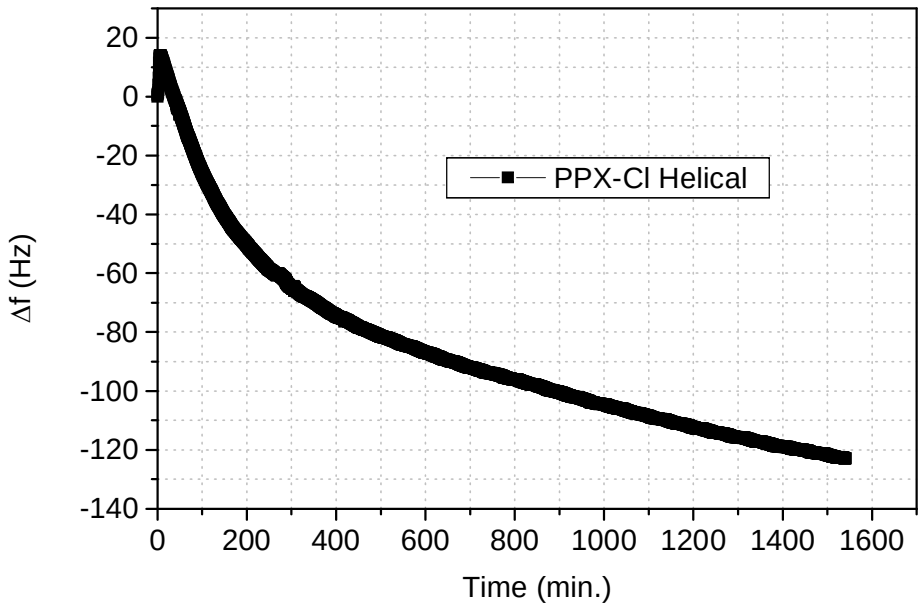

Figure 3 - Frequency over Time Measured by QCM for .289 µM [BSA] bulk solution and a PPX-Cl Helical film

Isotherms could then be compiled tracking such a negative frequency shift for each BSA solution concentration. Below are the isotherms for all three samples.

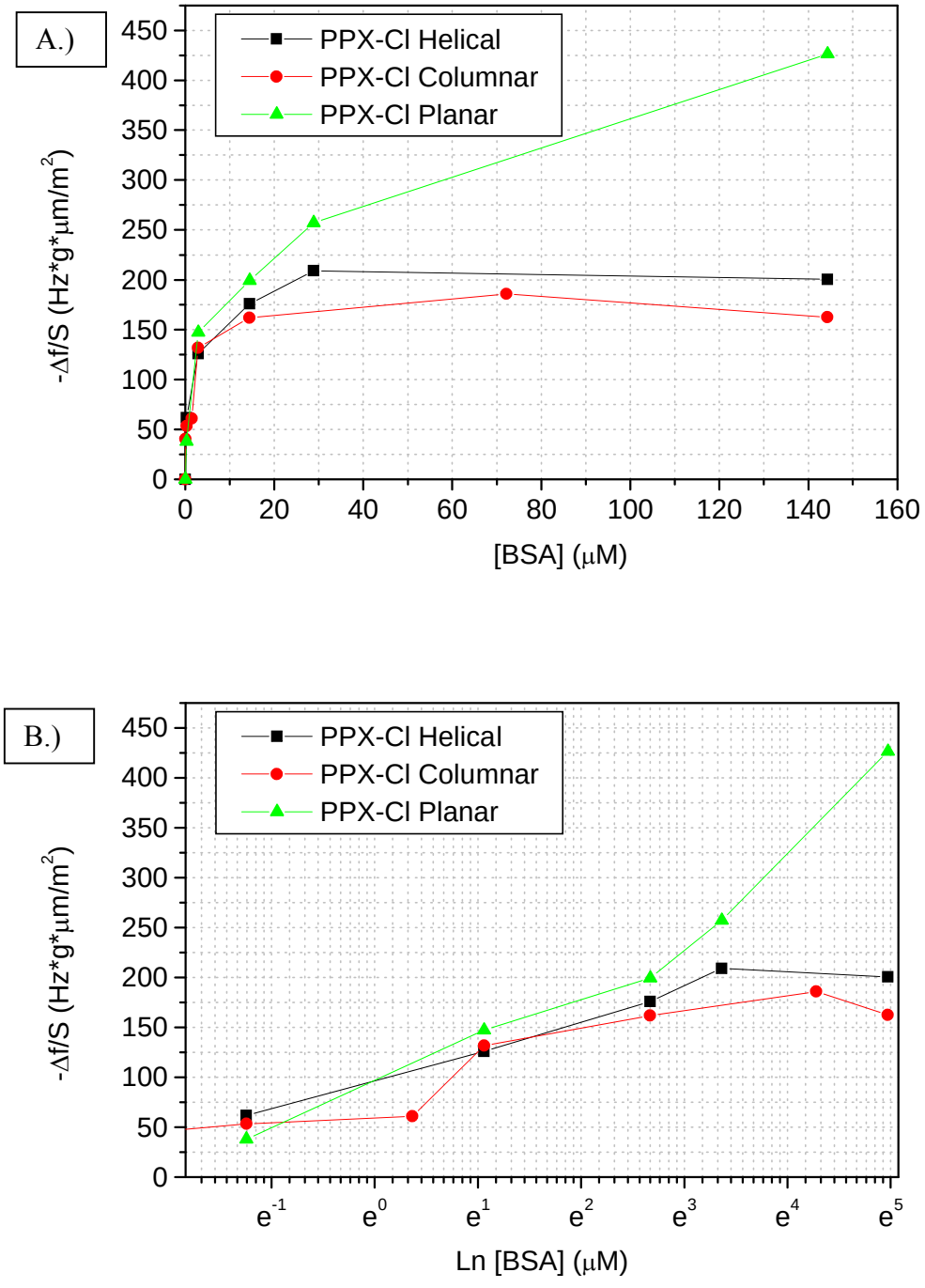

Figure 4 - This figure shows the isotherms for all three PPX samples. The vertical axis displays the negative change in frequency (-Δf) divided by the BET surface area (S) of each film while the horizontal axis displays BSA concentration on A.) a linear scale and B.) a logarithmic scale.

Each curve was then fit to a Langmuir isotherm using the Langmuir equation (Equation 5). In this case, since Equation 3 dictates a linear relationship between the negative frequency shift and adsorbed mass, Γ will simply be represented by $-\Delta f$. Concentration, c, corresponds to the concentration of BSA in the test solution as measured in μM. The curve fitting was performed by the computer software package Microcal Origin, version 5.0. To do the fitting, the curve was normalized such that each side of the Langmuir equation was divided by the known value of Γ_{max}. The following graph and table summarize the results of the Langmuir fitting.

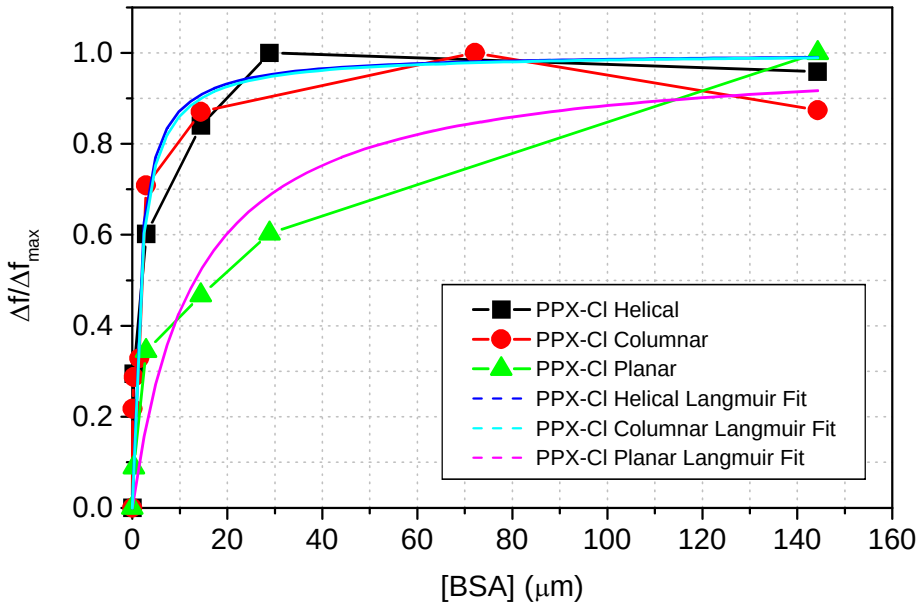

Figure 5 – The normalized isotherms for the three morphologies of PPX-Cl along with their corresponding Langmuir fit curves.

Film Type	Langmuir Constant (K) (M^{-1})	Error (M^{-1})	Chi-square (χ^2)
PPX-Cl Helical	6.9005×10^5	$+/- 1.8776 \times 10^5$	0.00572
PPX-Cl Columnar	6.2481×10^5	$+/- 1.8722 \times 10^5$	0.01268
PPX-Cl Planar	0.7628×10^5	$+/- .205 \times 10^5$	0.00981

Table 2 – Summary of the values resulting from the Langmuir fitting.

To determine the potential correlation between surface area and Langmuir constant, the following table was compiled comparing previously known values of BET surface area to Langmuir constants.

Film Type	BET Surface Area ($m^2g^{-1}\mu m^{-1}$)	Langmuir Constant (M^{-1})
PPX-Cl Helical	2.0948	6.9005×10^5
PPX-Cl Columnar	1.9855	6.2481×10^5
PPX-Cl Planar	0.3757	0.7628×10^5

Table 3 – Comparison of surface area and Langmuir constants for the different morphologies of PPX-Cl. BET surface area is normalized with respect to film thickness.

For the purpose of determining the effects of viscosity on the frequency shifts, resistance values were also measured. The change in resistance for each concentration was determined in the same fashion as the change in frequency. The graphs on the following page contain the change in resistance corresponding to each tested concentration for the three types of PPX.

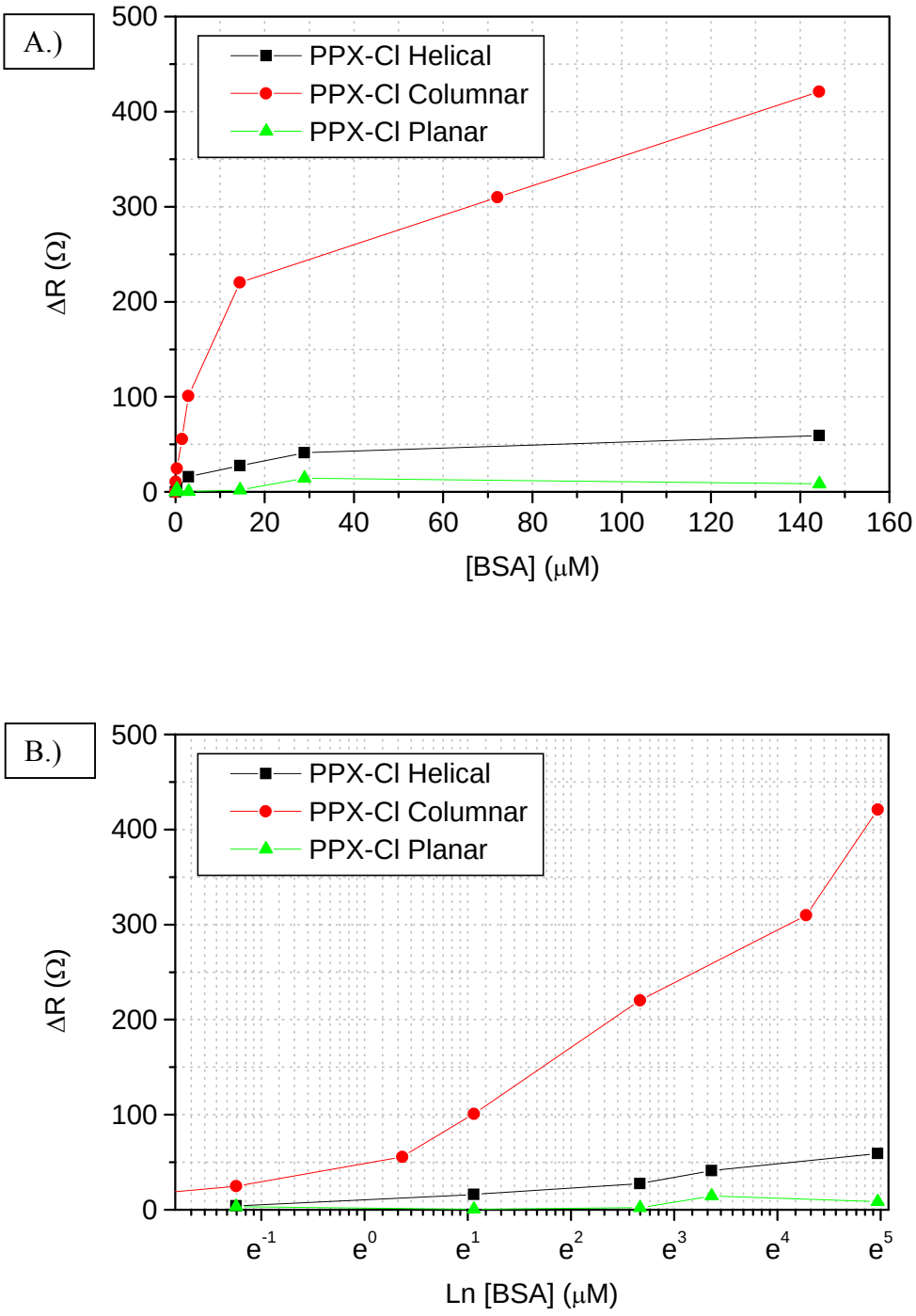

Figure 6 - This graph shows the change in resistance for each concentration of BSA solution tested. Displayed on the graph are the results for all three types of PPX tested on A.) a linear scale and B.) a logarithmic scale.

The graph below compares the change in resistance to the change in frequency for each of the PPX samples. This was done in order to determine the effect the change in resistance would have on the frequency shift.

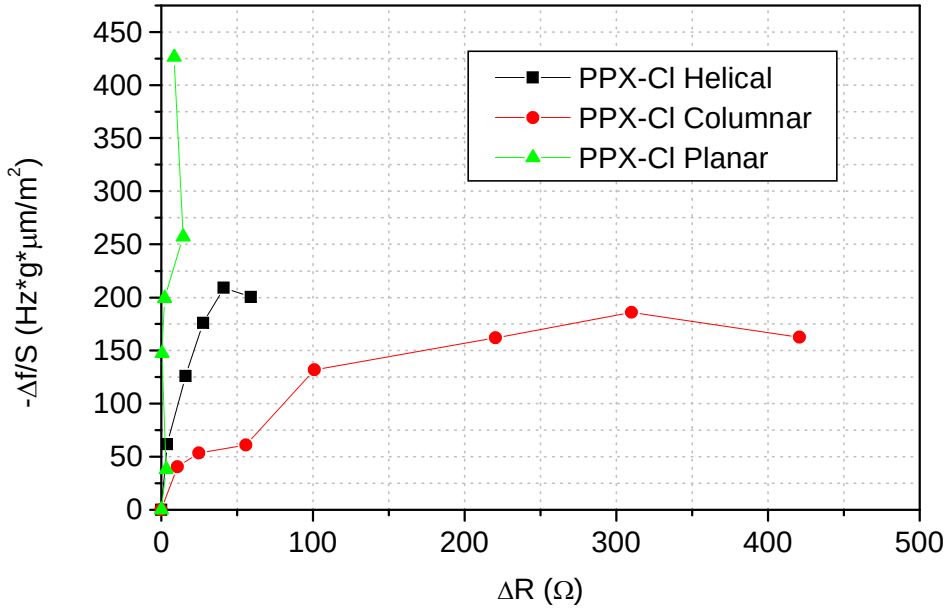

Figure 7 - This graph shows the change in frequency normalized with respect to surface area versus the change in resistance for each sample.

2.2 - Discussion

The QCM protein adsorption data compares three different morphologies of PPX-Cl. The important measurements taken and recorded were the changes in frequency and resistance. It is known from the Sauerbrey equation that a drop in frequency corresponds to an increase in adsorbed mass. This relation holds for vapor and liquid loading situations, although in the case of liquid loading the viscous coupling of the liquid also contributes to the frequency shift. Since resistance is directly proportional to viscosity by Equation 4, resistance measurements were taken to account for this effect.

Figure 3 shows the frequency readings taken by the QCM for the first test taken. It shows an early frequency drop followed by an equilibrium state. The curve appears similar to the situation described by Langmuir in the transient case and is thus expected. The frequency drop is expected by the Sauerbrey equation and corresponds to an increase in the mass on the surface. Though there are other factors influencing the frequency shift, those will be accounted for in the measurement of resistance. The protein successfully adsorbs to the surface because the PPX-Cl surface is a hydrophobic surface. The literature reviewed suggests that BSA has a higher affinity for hydrophobic surfaces because the protein can change its conformation in order to expose its hydrophobic parts and expel the water between the surface and the protein. The initial increase in the graph is due to the process of taking the crystal holder out of one solution and placing it in another. Since the focus of this data is not the kinetics of adsorption, no further discussion of the transient data is here included.

Figure 4 shows a comparison of the adsorption isotherms for the three samples. In each case some initial increase in frequency shift is followed by a sort of plateau in the data. By Equation 3, an increase on this graph corresponds to an increase in adsorbed

mass. The pattern of an initial increase in adsorption followed by a plateau is consistent with Langmuir type protein adsorption. In such an adsorption pattern, the protein adsorbs to the surface progressively more as the protein solution concentration increases until the active sites for protein adsorption are filled. At this point the film is saturated, or at equilibrium. No further adsorption occurs at that point. The plots on the logarithmic scale conform to a similar qualitative shape as other Langmuir isotherms obtained using QCM (see for example [19]).

The data in Figure 4 is of interest because it gives information about the effect of surface area on protein adsorption. The frequency shifts are normalized with respect to surface area. Even though the adsorption affinities based on frequency shift values alone show noticeable increases from planar to columnar to helical morphologies, as will be shown later in the discussion of Langmuir fitting, when normalizing with respect to surface area the planar film shows the largest frequency shift followed by the helical and columnar samples. This suggests that the increase in adsorption affinity is due to the increase in surface area caused by the change in morphology. The surface area causes such an increase because there are more active sites where more surface area is present and there is no change in surface chemistry. The fact that the planar sample's frequency shifts when normalized with respect to surface area are greater than those of the nanostructured samples may suggest that BSA adsorbs more easily to the planar surface apart from the surface area differences. Further tests would have to be performed to determine if and why this would be the case. The comparison of the actual values of surface area and adsorption affinity is contained in Table 3 and will be discussed shortly. This data then suggests that creating nanostructures of a polymer is a way to enhance the

adsorption or loading capacity of that polymer as more active sites are created by a greater surface area. The drop in negative frequency shift at higher concentrations for the nanostructured samples is possibly due to the aggregation of loosely bound proteins with aggregates in BSA solution, commonly observed at higher concentrations of BSA [22]. This causes the BSA to desorb from the surface and thus the drop in negative frequency shift.

Figure 5 simply shows the Langmuir fit for the three samples using Equation 5. The corresponding tables, Table 2, show the actual calculated values of the Langmuir constants. It can be seen from Table 2 that the Langmuir adsorption value calculated for the helical sample is highest, followed by the columnar and a significantly lower planar value. Each of these Langmuir constants for BSA is within an acceptable range of agreement with the literature (see for example [18]). Since the Langmuir constant is the equilibrium constant for the protein adsorption reaction, a higher Langmuir constant indicates a greater affinity for adsorption. The Langmuir constants thus verify that the adsorption affinity of BSA is greatest for PPX-Cl helical and least for PPX-Cl planar.

Table 3 then compares the BET surface area to adsorption affinity as expressed in the Langmuir constant. The results indicate that where surface area increases and surface chemistry remains the same, protein adsorption increases. It shows that from a PPX-Cl planar sample to a PPX-Cl columnar sample there is a ~420% increase in surface area corresponding to a ~700% increase in Langmuir constant. From the PPX-Cl planar sample to a PPX-Cl helical sample there is a ~450% increase in surface area corresponding to a ~800% increase in Langmuir constant. From the PPX-Cl columnar sample to the PPX-Cl helical sample there is a ~5% increase in surface area

corresponding to a ~10% increase in Langmuir constant. This lends further quantitative support to the concept that nanostructuring PPX enhances protein adsorption by increasing the surface area of the polymer.

After considering the frequency shift for each concentration, data was also compiled to examine the relationship between changes in resistance and BSA concentration. Resistance is not normalized with respect to surface area because it assumed that the viscous effects that damp oscillations only occur on the surface, since trapped liquid is known to oscillate with the surface [23]. Figure 6 shows a greater increase in resistance for higher concentrations of BSA solutions. This is due to the greater affect of viscosity and density of the BSA solution [18]. It also shows a greater increase in resistance for the columnar sample than for the helical, and a greater increase in resistance for the helical sample than the planar. This suggests the possibility of greater viscous effects on the columnar sample.

To consider the relationship between the change in resistance and the change in frequency the two were plotted in Figure 7. This helps to qualitatively determine how viscous or rigid the adsorption is by seeing how much the observed frequency shift in the isotherms is affected by a change in resistance, which is caused by viscous affects. In Figure 9, a more vertical line indicates more rigid adsorption since the frequency shift is occurring apart from a change in resistance. Conversely, a more horizontal line indicates a frequency shift caused largely by viscous coupling. It can then be seen that the rigidity of adsorption in decreasing order goes from planar to helical to columnar samples. In fact, between the last two points on Figure 7 for the planar sample there is a decrease in resistance. This corresponds to a further rigidifying of the layer [16].

While the planar and helical samples demonstrate relatively similar rigidity of adsorption, the data for the columnar film suggests significantly enhanced viscous effects and less rigid loading. Further study would be required to determine the cause of this. More trials of the columnar sample would need to be done to show that this is a real, repeatable, phenomenon. The columnar sample is not uniform throughout the surface in the same way the helical and planar samples are, so this could impact rigidity in some way, but further experimentation would be required to determine what causes the more viscous nature of adsorption for the columnar sample.

Chapter 3: Conclusion

Protein adsorption studies were performed on three morphologies of PPX-Cl, using BSA as a test protein. Adsorption was quantified by QCM. The results showed that for concentrations of BSA solution ranging from .07213 to 144.25 μM BSA successfully adsorbs to PPX-Cl surfaces in a Langmuir adsorption pattern with Langmuir constants equal to 6.9005 x 10^5 M^{-1}, 6.2481 x 10^5 M^{-1}, and .7628 x 10^5 M^{-1} for helical, columnar, and planar samples respectively. The results indicate that this increase in protein adsorption affinity is directly related to the increase in surface area caused by the nanostructured design of the helical and columnar samples. Due to ~420% and ~450% increases respectively in surface area over planar PPX, helical and columnar samples of PPX enhance protein adsorption affinity by ~800% and ~700% respectively over planar PPX. The results also show the most rigid adsorption to occur in the helical and planar morphologies. The best combination of rigid adsorption and adsorption affinity then is the helical sample of PPX. Since increasing surface area increases protein adsorption, the major advantage of PPX as a platform to control protein adsorption is the ability to alter its surface area by simply altering its morphology.

Such design considerations are a helpful conclusion and also give a future path for research: studying protein adsorption mechanism in a nanoporous polymer. This study showed that adsorption could be enhanced by nanostructuring, but it was beyond the scope of this study to understand what conformational changes etc. affect protein adsorption for a nanostructured polymer. Such a study could also look into the affects of the nanostructures on QCM measurements in more depth than this study was able to.

It could also be worthwhile to test a controlled drug release platform with all design considerations in place. Since QCM has proven to be a viable technique for measurement of loading, it should be tested for measurement of release as well. A good future experiment then would be to test helical PPX loading and release of some test drug using QCM. Such an experiment would give more definitive verification of the design guidelines concluded in this study. Since PPX can also be tuned in terms of its hydrophobicity or hydrophilicity by changing the precursor of PPX used, the effects of surface chemistry on loading and release could also be tested.

With such definitive verification of the important design guidelines in creating a valid method of controlling protein adsorption, a potential future path of research would be growing cells on the film and testing the effect of surface area on cell adhesion and growth. The PPX could also be patterned on a surface and used to load and release growth factors or genes. In these cases it can be investigated for its use in cell patterning and tissue engineering.

References

1. Andrade, J.D. ed. (1985) *Surface and Interfacial Aspects of Biomedical Polymers, Volume 2: Protein Adsorption.* New York, NY: Plenum Press.
2. Demirel, M. C. (2008). *Colloids and Surfaces*, *321*, 121-124.
3. Sauerbrey, G. (1959) *Zeitschrift für Physik A Hadrons and Nuclei, 155(2),* 206-222.
4. Martin, S.J., Granstaff, V.E., Frye, G.C. (1991) *Analytic Chemistry, 63,* 2272-2281.
5. Kundt, A. (1886) *Annals of Physics, 27,* 59.
6. Hawkeye, M. H., & Brett, M. J. (2007). *The Journal of Vacuum Science and Technology A*, *25(5*), 1317-1335.
7. König, H., Helwig, G. (1950) *Optik (Stuttgart), 6*, 111.
8. Callister, W. D. (2007). Phase Transformations in Metals. In *Materials Science and Engineering An Introduction* (pp. 311-357). New York, NY: John Wiley & Sons, Inc.
9. Demirel, M. C., E. So, T. M. Ritty, S. Naidu, and A. Lakhtakia. (2006) *Journal of Biomedical Research Materials-B*, *81B*, 219-223.
10. Centinkaya, M., S. Boduroglu, and M. C. Demirel. (2007) *Polymer, 48,* 4130-4134.
11. Boduroglu, S., Cetinkaya, M., Dressick, W. J., Singh, A., & Demirel, M. C. (2007). *Langmuir*, *23*, 11391-11395.
12. Malvadkar, N., Mangan, A., Boduroglu, S., Wang, H., & Demirel, M. C. (2009). *European Coating Journal*, *1*, 40-44.

13. Purcell, B. *Master's Thesis* (2008). Department of Engineering Science and Mechanics, The Pennsylvania State University. Supervisor: Professor Dr. Melik C. Demirel.
14. Gordon, J.G. II, Kanazawa, K.K. (1985) *Analytic Chemistry, 57,* 1770-1771.
15. Langmuir, I. (1916) *Journal of the American Chemical Society, 38* (11), 2221-2295.
16. Marxer, C.G., Coen, M.C., Schlapbach, L. (2003) *Journal of Colloid and Interface Science, 261,* 291-298.
17. Roach, P., Farrar, D., Perry, C.C. (2005) *Journal of the American Chemical Society, 127,* 8168-8173.
18. Kaufman, E.D., Belyea, J., Johnson, M.C., Nicholson, Z.M., Ricks, J.L., Shah, P.K., Bayless, M., Pettersson, T., Feldoto, Z., Blomberg, E., Claesson, P., & Franzen, S. (2007) *Langmuir, 23,* 6053-6062.
19. Kao, P.; Patwardhan, A.; Allara, D,; Tadigadapa, S. (2008) *Journal of Analytic Chemistry, 80(15),* 5930-5936.
20. Kao, P., Allara, D., Tadigadapa, S. (2009) *Measurement Science & Technology*, *20(12),* 1-9.
21. Malvadkar, N.A. (2010) *Doctoral Dissertation*. Department of Engineering Science and Mechanics, The Pennsylvania State University. Supervisor: Professor Dr. Melik C. Demirel.
22. Norde, W., Giacomelli, C.E. (2000). *Journal of Biotechnology, 79(3),* 259-268.
23. McHale, G., Newton, M.I. (2004). *Journal of Applied Physics, 95(1),* 373-380